Letter Vol. 47, No. 23 / 1 December 2022 / *Optics Letters* 6197

Optics Letters

Maximization or leveling: characterization of the trade-offs for the transmission throughput in ultrawideband optical transmission

Anastasiia Vasylchenkova,[1,*] Eric Sillekens,[1] Robert I. Killey,[1] and Polina Bayvel[1]

[1] *Optical Networks Group, Department of Electronic and Electrical Engineering, University College London, Torrington Place, London WC1E 7JE, UK*

**Corresponding author: a.vasylchenkova@ucl.ac.uk*

Received 11 July 2022; revised 1 November 2022; accepted 2 November 2022; posted 2 November 2022; published 28 November 2022

In ultrawideband transmission, the overall noise comes from the amplification, fiber properties at different wavelengths, and stimulated Raman scattering, and its impact on channels across transmission bands is different. This requires a range of methods to mitigate the noise impact. Performing channel-wise power pre-emphasis and constellation shaping, one can compensate for the noise tilt and attain maximum throughput. In this work, we study the trade-off between the goals of maximizing the total throughput and leveling the transmission quality for different channels. We use an analytical model for multi-variable optimization and identify the penalty from constraining the mutual information variation.

https://doi.org/10.1364/OL.470105

Introduction. Increasing the transmission bandwidth in optical fiber communications is a promising and cost-efficient way of increasing throughput to meet the growing data demands [1,2]. There are numerous studies of communication systems, covering conventional (C-) and long-wavelength (L-) bands, including commercially available amplification and transceiver devices. However, increasing bandwidth beyond the C+L wavelength ranges is still at the research stage [3]. The main obstacles in achieving ultrawideband transmission come from the frequency-dependent properties of channel parameters and inter-channel interactions.

In an optical transmission system, different channels may be designated for different users, so that any significant difference in the quality of transmission (QoT) across the bandwidth is undesirable. For a larger number of channels, the accumulated nonlinear channel interference dominates among other factors impacting the QoT degradation. Therefore, the currently applied nonlinearity mitigation methodologies are no longer valid. To maximize total throughput, these effects must be carefully estimated and taken into account. Given the considerable variation in link parameters across wavelength, equalizing the transmission quality is achievable only through the channel-wise manipulation of modulation parameters [4,5]. Optimal resource allocation, aiming at a flat QoT profile, is a computationally heavy multi-variable optimization task.

In ultrawideband scenarios, when more densely spaced channels are used, the QoT metrics can vary significantly from channel to channel. Therefore, these two tasks—achieving maximum throughput and maintaining a flat transmission quality profile—are in competition. Typically, when mutual information (MI) varies noticeably between channels (up to 3 dB in our simulations), it leads to a better total MI than in the case of uniform MI distribution. This trade-off is exacerbated in the ultrawideband scenario, and therefore, is the focus of this Letter.

Because of the nature of the optimization problem, given the variation in parameters over the transmission bandwidth and modulation parameters tuning, numerical simulations are not suitable because of their computational complexity. Instead, for the performance evaluation and monitoring, numerically integrable or closed-form analytical models must be used to estimate the impact of impairments [6,7]. Such models link the input system parameters and output communication quality. We note here that for the analysis in this work, the conventional analytical models (i.e., those not accounting for channel interaction via Raman scattering and modulation format [6]) are not applicable, as they cannot capture these effects crucial for the ultrawideband scenario [7].

To compensate for the variation in fiber properties over the bandwidth, different types of adjustments, such as power pre-emphasis and constellation shaping, are widely used, see [5,8]. Power pre-emphasis aims to reduce penalties coming from the uneven noise distribution, caused by the amplification and link impairments. When power manipulation is not sufficient, or noise becomes power-dependent, constellation shaping of individual channels is applied to make better use of the less distorted carriers.

The Gaussian noise (GN) model approach is an effective tool for estimating the signal-to-noise ratio (SNR) at the receiver [6]. The conventional GN model [6] can be expanded to account for non-uniform fiber attenuation, dispersion, and interchannel stimulated Raman scattering (ISRS) [7,9]. These effects are the main sources of impairment in the case of ultrawideband transmission, especially when channels in the S-band are also occupied [3,4,10].

Through the combination of numerical fitting of the solutions of Raman equations, the ISRS GN model and non-convex problem optimization, we can confidently analyze and optimize the transmission system with full occupancy of S-, C-, and L-bands (20 THz in total), for an arbitrary launch power and modulation format. The conventional approach to this type of optimization is to maximize the total information rate metric, while the importance of equalizing and maintaining the capacity of the individual channels is often ignored [4,5].

In this work, we use the ISRS GN model to study the trade-off between maximization and flattening of the transmission throughput for the S+C+L transmission, to quantify the gain–penalty balance for different optimization strategies. The launch power and constellation shape (both on a channel-by-channel basis) are varied and the optimization results for different link lengths are analyzed. These two optimization techniques are widely applied to design ultrawideband systems [5,8]. We use mutual information as a measure for the channel throughput and consider both the total MI for all channels and how the per-channel MI varies over the transmission bandwidth. This allows quantifying the available margins in the design of transmission systems with a high total information rate, yet sufficient QoT for individual users/channels.

QoT estimation via the ISRS GN model. Employing SNR as a metric for QoT and for further estimation of data throughput, we use the ISRS GN model, adapted to account for an arbitrary power profile and constellation shape [7]. The conventional GN model is based on the first-order perturbation method with respect to the fiber nonlinearity. The GN model determines the contribution of nonlinear impairments to ith channel total SNR, defined as

$$\mathrm{SNR}_i^{-1} = \mathrm{SNR}_{\mathrm{ASE}}^{-1} + \mathrm{SNR}_{\mathrm{TRx}}^{-1} + \mathrm{SNR}_{\mathrm{SPM},i}^{-1} + \sum_{k\neq i}^{N_{\mathrm{ch}}} \mathrm{SNR}_{\mathrm{NLI},ik}^{-1}. \quad (1)$$

The GN model provides an estimate for both self- and cross-phase modulation (SPM and XPM, respectively) effects [6,7]. ISRS leads to channel power transfer and to a tilted SNR profile across the transmission window. The contribution from ISRS using the system of Raman equations to describe the power transfer between channels during the propagation in the fiber can be added using the approach from [7,9].

In this work, we focus on the interaction between the constellation distribution and launch power within the ISRS GN model. The SPM contribution to the SNR can be expressed as

$$\mathrm{SNR}_{\mathrm{SPM},i}^{-1} = \eta_{\mathrm{SPM}} P_i^2, \quad (2)$$

while the XPM contribution can be given as

$$\mathrm{SNR}_{\mathrm{NLI},ik}^{-1} = (\eta_{\mathrm{GN}} + \eta_{\mathrm{corr}}\Phi) P_k^2. \quad (3)$$

The η_{SPM}, η_{GN}, and η_{corr} are the nonlinear coefficients for SPM, XPM, and the XPM modulation format correction, respectively. In this work, we used the expressions found in Ref. [7, Eq. (16)] for the results presented. The second term in Eq. (3) accounts for the impact of shaped constellations via its statistical characteristics called (excess) kurtosis Φ—its central normalized fourth-order moment. It measures the deviation of a given constellation from the Gaussian one, assumed by default in the GN model, for which $\Phi = 0$. Another extreme is the QPSK constellation, for which $\Phi = -1$, for all variety of practically possible constellation probabilities Φ stays within this range.

Table 1. Transmission Parameters for ISRS GN Modeling and SNR Calculation

$\mathrm{SNR}_{\mathrm{TRx}}$	23 dB	spacing Δf	50 GHz
L_{span}	80 km	dispersion D	18 ps/km/nm
dispersion slope S	0.067 ps/km/nm^2	nonlinearity γ	1.3 1/W/km
S band λ range	1465–1520 nm	*S band* NF	7 dB
C band λ range	1530–1565 nm	*C band* NF	4 dB
L band λ range	1570–1623 nm	*L band* NF	6 dB

To extend the accuracy of these expressions for the transmission bandwidth beyond 15 THz, one has to fit the numerical solution of the Raman equations for a given launch power profile [7,9]. Therefore, the per-channel power is not completely factorizable in the SNR expressions above, and the nonlinear coefficients η are functions of the launch power, as well as other signal properties (e.g., per-channel bandwidth), and other fiber properties, like attenuation and nonlinearity [7].

Although the perturbation method in the GN model provides explicit expressions for the nonlinearity contribution to the SNR [6,7], efficient optimization of system performance is difficult because it is a non-convex optimization problem with a large number of system parameters.

In this study, we use the experimental amplification scheme parameters, taken from [3,10], in particular, the value of the noise figure (NF). In the S-band, the noise performance is worse than in the C- and L-bands (Table 1). For optimization purposes, we represent the launch power as a smoothly varying polynomial function *in each band separately*. Having this polynomial function allows for a wide range of power values to compensate for possible impairments, while keeping the number of parameters low (since the number of coefficients is much smaller than the number of channels).

Atop of the launch power pre-emphasis, we apply probabilistic shaping to reach higher MI values. As in the case of probabilistic shaping, we keep the coordinates from the square 256-QAM modulation format and match its points with the probability determined by the distance to that point from the origin. To try various constellation shapes, we use the probabilistic shaping with two turning parameters $\nu_{1,2}$. The probability of a constellation point is then

$$p(x_i) = \frac{\exp(-\nu_1|x_i|^2 - \nu_2|x_i|^4)}{\sum_j p(x_j)}, \quad (4)$$

where the denominator is used for the normalization purposes [8]. This choice allows the operation over the desired range of $-1<\Phi<0$, with a feasible number of parameters. The variation of kurtosis Φ across the $\nu_{1,2}$ plane is plotted in Fig. 1.

For the given values of $\nu_{1,2}$ and launch power distribution, we use the closed-form ISRS GN model, Eqs. (1–3), to estimate the received signal SNR. Then, for a given constellation shape and SNR, we calculate MI over the transmission bandwidth.

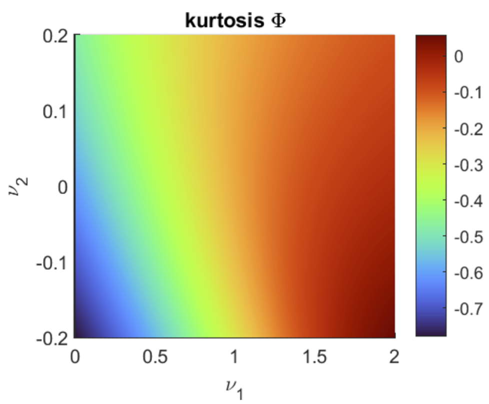

Fig. 1. Values of the constellation's kurtosis Φ, calculated for the landscape of probabilistic shaping parameters $\nu_{1,2}$.

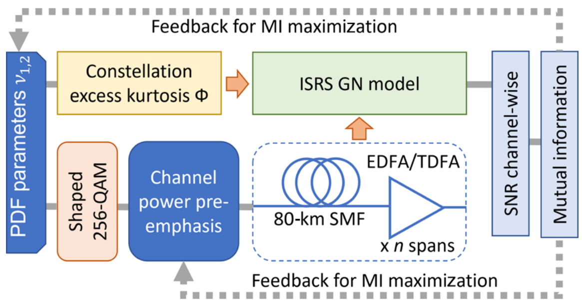

Fig. 2. Schematics of the analyzed transmission system and MI maximization procedure.

The schematic of the transmission scheme and optimization procedure are given in Fig. 2.

To study the trade-off between global MI maximization and maintain a flat MI profile (characterized by the MI variation ΔMI), we set the *constrained* optimization problem. Its cost function is the total throughput $\sum_i \mathrm{MI}_i$, while the maximum variation of the MI values $\Delta\mathrm{MI}=\max_{i,j}|\mathrm{MI}_i-\mathrm{MI}_j|$ is limited. For smaller ΔMI, so for a stronger constraint, power pre-emphasis can provide a smaller gain in terms of achievable total MI. In other words, flattening of the MI comes at the penalty in total MI. In this work, we quantify how constraint strength impacts the achievable total MI.

Results and discussion. For the throughput optimization, we modeled a state-of-the-art transmission system, with probabilistically shaped 256-QAM modulation of $N_{\mathrm{ch}} = 401$ WDM channels. The combined EDFA/TDFA amplification was included to cover the S, C, and L bands. The total number of channels was assumed to be 401, with 363 of them modulated, the remainder falling within spectral gaps of the amplification scheme. Fiber attenuation was modeled to be frequency-dependent and taken from the measurement of a Corning SMF-28 ULL fiber. In this work, we carried out the optimization for the different number of fiber spans, with all the spans assumed to be identical, recreating the optimal launch power profile at the beginning of each span by the gain flattening filter. This is done to show how maximization-flattening trade-off changes for different link lengths. Other relevant transmission parameters used in the simulations are listed in Table 1. For reference, the total data rate at the 1300 km link length, assumed to use polarization multiplexing, is 170 Tbps prior to the optimization, mainly extending the system from [11] to longer distances. The optimization allowed achieving up to 10% gain in terms of data rate. At shorter distances, the achievable data rate is larger and in reasonable accordance with the experimental advances, e.g., of 107 Tbps transmission at 300 km link length and 60% narrower total bandwidth [2].

The optimization was performed using the trust-region method [12], aiming for the maximization of the total MI with or without additional constraint. Therefore, we refrain from leveling the received power spectral distribution and focus on the actual objective, which is the total data throughput of the system. The trust region method can deal with nonlinear and non-convex functions, as required for the dependence between the coefficients of the launch power profile and the total MI. However, it requires seed values for input parameters. To apply it fairly, we use the outcomes of previous modeling studies in Ref. [10] when initiating optimization for $\nu_1 = \nu_2 = 0$. For the nonzero shaping parameters, we seed the optimizer with an outcome of the already computed optimal point for neighboring $\nu_{1,2}$.

First, we analyzed the difference between constrained and unconstrained MI maximization. Figure 3 shows the results for n=10 spans, this value is chosen for illustration purposes, the conclusions below are qualitatively the same for at least up to 20 spans where we performed the optimization. MI maximization is performed independently for each $\nu_{1,2}$ pair across the plane for a range of practical probability distributions: $0 \le \nu_1 \le 2$, $|\nu_2| \le 0.2$. Note that extreme cases of $\nu_2 \le 0$, $|\nu_2|>\nu_1$, according to Eq. (4), yields a noticeable preference to outer constellation points.

Figure 3 highlights the general trend that limiting the MI variation decreases the maximum achievable MI. For example, ΔMI=0.5 bit/4D, the maximum drops from 12 bits/4D to 9 bit/4D. We also see the overall similarity in optimal MI landscape on the $\nu_{1,2}$ space. We also found that the location of the extremum in the MI surface is unchanged for all studied ΔMI and all studied numbers of spans, meaning that the optimal constellation shape does not change with the transmission distance. The optimum corresponds to $\nu_1 \approx 1.5$, $\nu_2 \approx 0$.

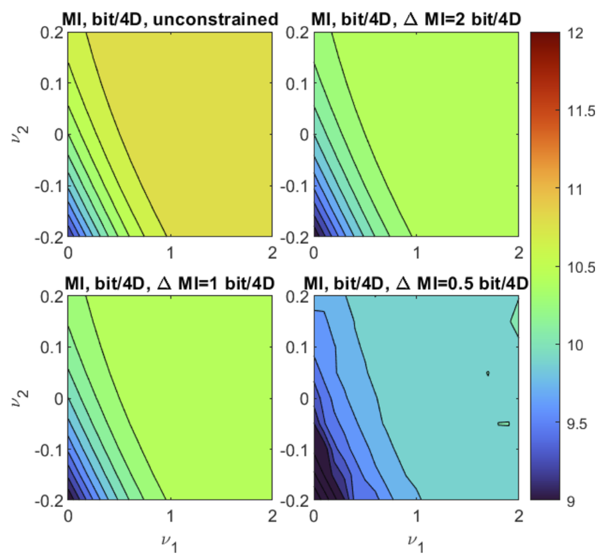

Fig. 3. Maximum total MI achievable for different constellation shapes (parameterized by $\nu_{1,2}$) via channel-wise power pre-emphasis. The results are given for different values of the constraint ΔMI, and for the unconstrained maximization. The results are given for the 10 span link with 800 km total length.

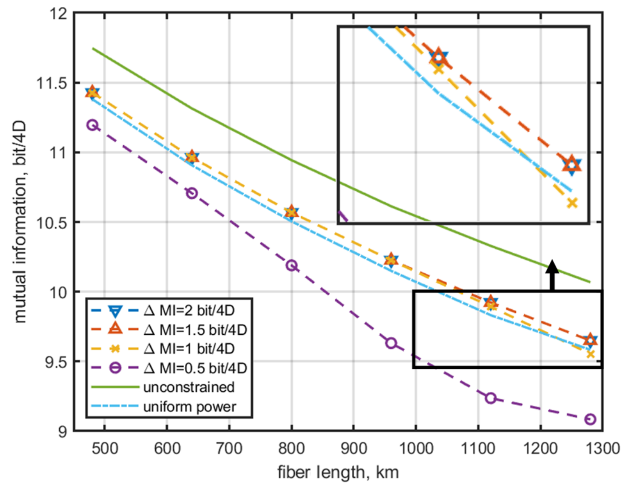

Fig. 4. Maximum achievable total MI as a function of fiber length for different values of the MI variation constraint ΔMI. The gain from pure probabilistic shaping (i.e., for constant launch power) is given for comparison.

The penalty from limiting MI variation for different numbers of spans is given in Fig. 4. The difference between the total achievable throughput with and without the MI constraint is approximately constant for all studied link lengths. This is not the case for the strongest constraint ΔMI=0.5 bit/4D, where the penalty grows for a longer link. We also note that there is no difference meaning that such a limit for MI limitation is not significant. Expanding the window for MI variation beyond ΔMI=1 bit/4D results in negligible gain in terms of MI achievable by power optimization.

For comparison, we show the dependence of the total MI on the number of spans achieved by a pure probabilistic shaping, without varying the launch power. In this case, the launch power is set spectrally uniform at the level maximizing the total MI, at approximately 0.5 dBm similarly to the analysis reported in Ref. [4]. For weaker constraints (ΔMI≥1 bit/4D), the achievable MI is higher than the values resulting from pure constellation shaping and uniform launch power for shorter links. In contrast, for longer links (1300 km and beyond), pure shaping outperforms constrained optimization. Having a tighter limit ΔMI=0.5 bit/4D, the channel-wise optimization cannot reach the values of MI, achievable by probabilistic shaping only.

The optimal launch power was sufficiently described by the polynomials of degree 4, and increasing the power of the fitting more brought marginal improvement only. Because of the ISRS power depletion and a variation in NF, for the unconstrained optimization, we receive a highly varying launch power per band, namely, P_S = 1 dBm, P_C =-2.5 dBm, and P_L=-4 dBm. In contrast, for the constrained optimization, the power values are closer, e.g., for ΔMI=0.5 bit/4D, the launch power varies between -0.5 dBm and 0.5 dBm. For the pure shaping gain presented in Fig. 4, we use the uniform launch power around -1.5 dBm which maximizes the total MI.

Conclusions. The ISRS GN model and its modulation format corrections provide an effective toolbox for ultrawideband transmission system analysis and design. It was used for an extensive optimization study to characterize the interplay between total MI maximization and the necessity to keep the variation of individual channel MI low. We applied the channel-wise power pre-emphasis and probabilistic shaping as optimization parameters. The results highlighted that aiming for less than ΔMI=1 bit/4D constraint for the transmission system with a total throughput of 170 Tbps can appreciably decrease the achievable MI below the shaping gain level. The penalty in terms of the total MI increases with the transmission distance. This effect is more noticeable for stronger constraint conditions (up to ΔMI=0.5 bit/4D). The constraint-caused MI gap tends to grow for a larger number of spans, so we can expect the trend to be maintained for longer links. Also, for larger distances and a tight constraint, the balance between NLI and ASE noise shifts toward the latter, slowing down the growth of the penalty from the constraint, as the descent of the ΔMI = 0.5 bit/4D line becomes gentler. With this study, we have identified how the constraint limits the achievable total throughput. This provides valuable insight into how to design and optimize ultrawideband optical fiber transmission systems.

Funding. Engineering and Physical Sciences Research Council (EP/R035342/1); Leverhulme Trust (ECR-2020-150).

Disclosures. The authors declare no conflicts of interest.

Data availability. Data underlying the results presented in this paper are available in Ref. [13].

REFERENCES

1. J. Renaudier, A. Arnould, A. Ghazisaeidi, D. Le Gac, P. Brindel, E. Awwad, M. Makhsiyan, K. Mekhazni, F. Blache, A. Boutin, L. Letteron, Y. Frignac, N. Fontaine, D. Neilson, and M. Achouche, J. Lightwave Technol. **38**, 1071 (2020).
2. J. Renaudier, A. Arnould, D. Le Gac, A. Ghazisaeidi, P. Brindel, M. Makhsiyan, A. Verdier, K. Mekhazni, F. Blache, H. Debregeas, A. Boutin, N. Fontaine, D. Neilson, R. Ryf, H. Chen, M. Achouche, and G. Charlet, in *Optical Fiber Communication Conference* (Optica Publishing Group, 2019) paper Tu3F.2.
3. L. Galdino, A. Edwards, W. Yi, E. Sillekens, Y. Wakayama, T. Gerard, W. S. Pelouch, S. Barnes, T. Tsuritani, R. I. Killey, D. Lavery, and P. Bayvel, IEEE Photonics Technol. Lett. **32**, 1021 (2020).
4. H. Buglia, E. Sillekens, A. Vasylchenkova, W. Yi, R. Killey, P. Bayvel, and L. Galdino, in *International Conference on Optical Network Design and Modeling (ONDM)* (IEEE, 2021), pp. 1–4.
5. A. Ferrari, A. Napoli, J. K. Fischer, N. Costa, A. D'Amico, J. Pedro, W. Forysiak, E. Pincemin, A. Lord, A. Stavdas, J. P. F.-P. Gimenez, G. Roelkens, N. Calabretta, S. Abrate, B. Sommerkorn-Krombholz, and V. Curri, J. Lightwave Technol. **38**, 4279 (2020).
6. P. Poggiolini, G. Bosco, A. Carena, V. Curri, Y. Jiang, and F. Forghieri, J. Lightwave Technol. **32**, 694 (2014).
7. D. Semrau, R. I. Killey, and P. Bayvel, J. Lightwave Technol. **37**, 1924 (2019).
8. E. Sillekens, D. Semrau, G. Liga, N. A. Shevchenko, Z. Li, A. Alvarado, P. Bayvel, R. I. Killey, and D. Lavery, in *Optical Fiber Communication Conference* (IEEE, 2018), paper M3C.
9. D. Christodoulides and R. Jander, IEEE Photonics Technol. Lett. **8**, 1722 (1996).
10. D. Semrau, E. Sillekens, R. I. Killey, and P. Bayvel, in *2020 IEEE Photonics Conference (IPC)* (IEEE, 2020), pp. 1–2.
11. L. Galdino, D. Semrau, M. Ionescu, A. Edwards, W. Pelouch, S. Desbruslais, J. James, E. Sillekens, D. Lavery, S. Barnes, R. I. Killey, and P. Bayvel, J. Lightwave Technol. **37**, 5507 (2019).
12. R. H. Byrd, J. C. Gilbert, and J. Nocedal, Math. Program. **89**, 149 (2000).
13. A. Vasylchenkova, "Data accompanying Optics Letters 'Maximization or leveling: characterization of the trade-offs for the transmission throughput in ultrawideband optical transmission'," University College London: Version 2, 16 November 2022, https://doi.org/10.5522/04/21559311.v2.